

Cite this: DOI: 00.0000/xxxxxxxxxx

Designing Refractive Index Fluids using the Kramers–Kronig Relations[†]Tianqi Sai,^{a,b} Matthias Saba,^a Eric R. Dufresne,^b Ullrich Steiner,^{*a} and Bodo D. Wilts^{*a}Received Date
Accepted Date

DOI: 00.0000/xxxxxxxxxx

For a number of optical applications, it is advantageous to precisely tune the refractive index of a liquid. Here, we harness a well-established concept in optics for this purpose. The Kramers-Kronig relation provides physical connection between the spectral variation of the (real) refractive index and the absorption coefficient. In particular a sharp spectral variation of the absorption coefficient gives rise to either an enhancement or reduction of the refractive index in the spectral vicinity of this variation. By using bright commodity dyes that fulfil this absorption requirement, we demonstrate the use of the Kramers-Kronig relation to predictively dial-in refractive index values in water solutions that are otherwise only attained by toxic specialised liquids.

1 Introduction

The refractive index of a dielectric optical medium is typically considered to be an intrinsic property that is closely linked to the dipole moments of the atoms and molecules that constitute the optical medium¹. The tuning of optical substances – liquid as well as solid – is common place by either doping the optical medium with high dipole-strength substances or by designing the chemical nature of the medium. The latter is for example exploited in the manufacture of liquids with high refractive indices that are used to increase the resolution in photo-lithography. Commercial immersion liquids with refractive indices beyond 1.60 are usually composed of methylene iodide, arsenic tribromide, arsenic disulfide, sulfur and selenium^{2–6}. While widely used in industrial applications, these immersion liquids are toxic and the rational design of novel liquids based on non-toxic materials would be useful. This is in particular relevant for biological and medical high-resolution imaging, such as total internal reflection fluorescence microscopy⁷, where high-index optics based on sapphire lenses facilitate super-resolution⁸.

To this end, it is useful to consider the fundamental theories of the propagation of light. Based on the finite speed of the propagation of light, the consequences of causality on mathematical relationships of optical constants was considered nearly 100 years ago: For the scattering of light from an object, causality requires that “no scattered wave can exist before the incident wave has reached the scattering center”⁹. Based on this consideration,

Kramers¹⁰ showed that the refractive index of a medium can be calculated from its absorption spectrum. Combined with Kronig’s¹¹ argument that a “dispersion relation is a sufficient and a necessary condition for strict causality to hold” this establishes the well-known Kramers-Kronig relations, which constitute the connection between the in- and out-of-phase responses of a system to sinusoidal perturbations. Mathematically, the Kramers–Kronig relations connect the real and imaginary parts of any complex function that is analytic in the upper half-plane and vanishes sufficiently fast for large arguments^{9,12}. Physically, such a function corresponds to an analytical linear response function of finite width in the time domain.

For an optical system with a complex refractive index $\mathbf{n} = n + i\kappa$, with $n(\omega)$ the ‘real’ refractive index and $\kappa(\omega)$ the extinction coefficient, both of which vary with the angular frequency of the electromagnetic field ω , the Kramers–Kronig relation can be written as⁹

$$n(\omega) - 1 = \frac{2}{\pi} \mathcal{P} \int_0^\infty \frac{\omega' \kappa(\omega')}{\omega'^2 - \omega^2} d\omega', \quad (1)$$

where \mathcal{P} denotes the Cauchy principal value of the integral.

When used in spectroscopy, it is useful to write eqn (1) in terms of the optical wavelength $\lambda = 2\pi c/\omega$, where c is the speed of light. A substitution of the integration variable yields

$$\Delta n(\lambda) = n(\lambda) - 1 = \frac{2}{\pi} \mathcal{P} \int_0^\infty \frac{\kappa(\lambda')}{\lambda' \left(1 - \left(\frac{\lambda'}{\lambda}\right)^2\right)} d\lambda'. \quad (2)$$

An additionally requirement of the Kramers-Kronig relation is the superconvergence theorem⁹, leading to

$$\int_0^\infty \frac{\Delta n(\lambda')}{\lambda'^2} d\lambda' = \lim_{\lambda \rightarrow 0} \left[\frac{\pi \kappa(\lambda)}{\lambda} \right] = 0, \quad (3)$$

^a Adolphe Merkle Institute, University of Fribourg, Chemin des Verdiers 4, CH-1700 Fribourg, Switzerland. E-mail: ullrich.steiner@unifr.ch; bodo.wilts@unifr.ch

^b Department of Materials, ETH Zürich, Vladimir-Prelog-Weg 5, CH-8093 Zürich, Switzerland.

[†] Electronic Supplementary Information (ESI) available: Materials and Methods, Table S1 and Figs. S1–S4. See DOI: 00.0000/00000000.

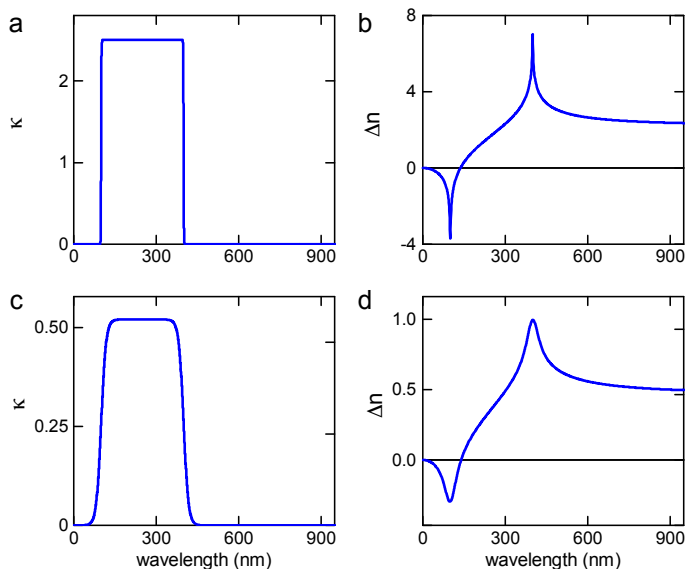


Fig. 1 Refractive index spectra, calculated by numerically solving eqn (2). (a) Hypothetical extinction spectrum confined to the 100–400 nm band. (b) Refractive index change Δn corresponding to (a). (c) Alternative hypothetical extinction spectrum and (d) corresponding Δn -spectrum. Similar plots with extinction spectra given by single Lorentzian peaks are shown in Fig. S3.

defining the asymptotic limit of the extinction coefficient κ , which is related to the experimentally measured absorption coefficient by

$$\alpha = \frac{4\pi}{\lambda} \kappa(\lambda). \quad (4)$$

The use of Kramers-Kronig relation in optics is extremely well established^{9,13–15}. It is often used to determine the spectral variation $n(\lambda)$ of an analyte from a measured absorption spectrum, and vice versa.

While identical in terms of the underlying physics, this work explores an alternative approach to create new high refractive index liquids with a designed optical response, by exploring the Kramers-Kronig relation. This concept was illustrated by the refractive index dispersion of pigments in biological samples^{14,15}, the oxygen saturation levels of human blood¹³, and the high refractive index materials in the wing scales of Pierid butterflies¹⁶.

2 Results and discussion

2.1 Conceptualisation of the Kramers-Kronig approach

Our concept is illustrated in Fig. 1. To explore the physical limits of the Kramers-Kronig effect, i.e. the relation between absorption and refractive index change, we assume a hypothetical pigment with a sharply defined boxcar-shaped absorption band of $\kappa=2.5$ in the 100–400 nm wavelength range (Fig. 1a). Fig. 1b shows that in this hypothetical case, Δn is very strongly enhanced: $\Delta n(400\text{ nm}) \approx 7$; $\Delta n(400\text{ nm}) - \Delta n(\infty) \approx 4.8$. A characteristic spectral feature of Δn is the long wavelength decay, the region of “normal” dispersion, which can be approximated by the Cauchy equation¹⁷

$$n_C = A + B/\lambda^2, \quad (5)$$

where $A = (2/\pi) \int d\lambda' \kappa(\lambda')/\lambda'$ and $B = (2/\pi) \int d\lambda' \lambda' \kappa(\lambda')$ can be used as fit parameters. Note that each spectral feature in the the absorption spectrum gives rise to a long-wavelength Cauchy decay, which are additive⁹, ultimately determining the overall refractive index variation of a given material in each transparent wavelength window.

While perhaps somewhat unrealistic, Fig. 1a,b illustrate the scope of our approach. Importantly, the enhancement of Δn extends to wavelengths where the absorption coefficient is practically zero. The strong enhancement close to, but above, the absorption band makes this idea particularly attractive in applications where only narrow-band illumination is required, e.g. telecommunication¹⁸ or lenses for immersion lithography¹⁹. By carefully selecting a short-wavelength absorber, a high refractive index can be dialled-in in a controlled fashion.

Fig. 1c,d shows a prediction which is closer to physical parameters that can be achieved for liquids: an extinction coefficient $\kappa=0.52$ which corresponds to $\alpha \approx 10.3 \mu\text{m}^{-1}$ at $\lambda=630\text{ nm}$ of a 0.6 M Brilliant Blue solution in water (see below). In this simulation, the absorption edge was smeared-out over ca. 35 nm. Here, an overall refractive index enhancement of ≈ 1 is expected at 400 nm compared to the dye-free solution and a value of $\Delta n \approx 0.8$ at 430 nm, where the dye absorption has decayed to just a few percent of its maximal value. While perhaps not as impressive as the hypothetical case in Fig. 1b, this concept has the potential to enhance the refractive index of common liquids into the range commonly reserved to specialised toxic liquids³.

2.2 Food dyes for water-based refractive index fluids

To demonstrate the concept of refractive index tuning through the selection of an appropriate absorber, four commonly used non-toxic, water-soluble dyes were investigated: the triarylmethane dye “Brilliant Blue”, the azo dye “Allura Red”, the sulfonated “Quinoline Yellow”, and the arylsulfonate “Pyranine”. The chemical structure and IUPAC names are given in Fig. S1 in the Supplementary Information (SI). The first four dyes are common food colorants²⁰, while the last is a fluorescent coloring agent used in hair dye and text markers. All four are water-soluble, non-toxic commodity compounds.

To start our investigation, UV-Vis transmission spectra of all four dyes were acquired. Water solutions of the four dyes were prepared with series of concentrations c_d up to the solubility limit of the dyes (between 300 mM and 600 mM). The spectral absorption coefficients were then determined according to the Beer-Lambert law, shown in Fig. 2. The absorption coefficient of Allura Red shows rather broad spectral peaks with a broad decay toward long wavelengths and a peak absorption at about 500 nm. In contrast, Brilliant Blue, Quinoline Yellow, and Pyranine show sharper spectral decays towards long wavelength at 630 nm, 412 nm, and 428 nm, respectively, which combine the prerequisite for a strong Δn enhancement at these wavelengths according to eqn (2) with the possibility to access a significant Δn -enhancement in the spectral domain where light absorption is insignificant (see Fig. 1). Particularly Brilliant Blue is an excellent candidate dye with an absorption coefficient of $17.25 \pm 0.04 \text{ M}^{-1} \mu\text{m}^{-1}$ at 630 nm.

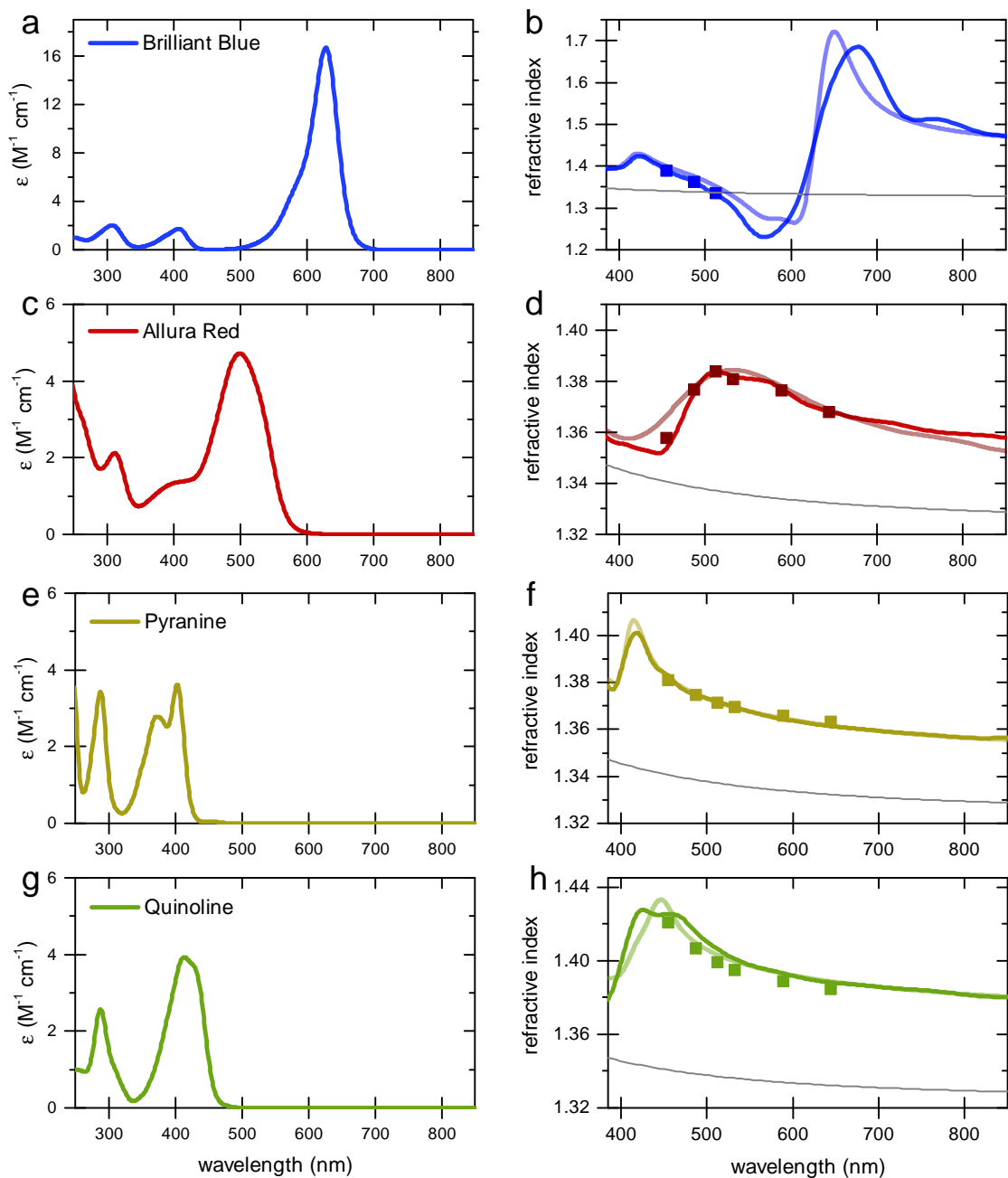


Fig. 2 Molar absorption spectra $\epsilon(\lambda) = \alpha(\lambda)/c_d$ (left column) and refractive index variation (right column) of the four dye solutions in water, (a,b) 0.6 M Brilliant Blue, (c,d) 0.3 M Allura Red, (e,f) 0.3 M Pyranine, and (g,h) 0.3 M Quinoline Yellow. In the right column, the solid lines and the square symbols are ellipsometry and refractometry measurements, respectively. The light coloured lines are calculated using the Kramers-Kronig relations. The refractive index variation of water (grey lines) is shown for comparison.

Spectroscopic ellipsometry was employed to measure the spectral variation $n(\lambda)$ of the various dye solutions, according to the protocol by Synowicki *et al.*²¹. In this method, dye solution drops are placed onto a rough glass substrate. The rough glass substrate enables the spreading of the water-dye solutions to provide a planar liquid surface and it suppresses the specular back reflection of the incident light beam from the liquid-substrate interface. Since only the phase relationship of the light reflected from the liquid-air surface is analysed, the ellipsometry data analysis is not very sensitive to the imaginary part of the refractive index κ . Therefore, only the real part of the refractive index $n(\lambda)$ was extracted from the ellipsometric data. To test the reliability of this approach, the variation of the refractive index of water was determined in the 400–1000 nm wavelength range and an agreement of better than 0.5% with literature data was found (Fig. S2 in the SI). As a further test of the measurement protocol, a 6-wavelength (455–655 nm) Abbe-refractometer was also used, with a measurement accuracy of refractive index of 4×10^{-4} .

The results of the ellipsometry and refractometry measurements for the highest concentration of the four dyes in water are shown in Fig. 2. A comparison with the spectral variation of the absorption curves bear out the qualitative variation of Δn of Fig. 1, i.e. all curves exhibit the signature predicted by the Kramers-Kronig relations.

To calculate the variation of $n(\lambda)$ from the absorption curves of Fig. 2, the limitations of the integration of eqn (2) have to be discussed. The prediction of the Kramers-Kronig relation is only precise if the variation of the extinction coefficient κ is known for the entire spectral wavelength range ($0 \rightarrow \infty$). Since this is generally impossible, we exploit the limiting properties of eqn (2) given by the Cauchy eqn (5).

Considering, for example, an absorption spectrum with two distinct spectral features (Fig. S3 in the SI), the integral in eqn (2) can be decomposed into two separate integrations, the results of which are then added to yield the overall spectral response $n(\lambda)$ ⁹. In the range of the long-wavelength absorption peak, the Δn -contribution of the short-wavelength absorption peak can be approximated by eqn (5), which can be added to the result of eqn (2).

In the absence of spectral information below $\lambda = 250$ nm, which strongly affects the long-wavelength variation of Δn , the following approach was therefore adopted.

1. Calculation of $\kappa(\lambda)$ from the absorption curves in Fig. 2, using eqn (4), setting $\kappa = 0$ for $\lambda < 250$ nm and $\lambda > 1000$ nm.
2. Integration of eqn (2) to obtain $\Delta n(\lambda)$.
3. Approximation of the refractive index variation of water n_{Cw} (Fig. S2 in the SI) by eqn (5).
4. Calculation of $n_{KK}(\lambda) = \Delta n(\lambda) + n_{Cw}(\lambda) + n_{Cd}(\lambda)$, with another Cauchy-type refractive index contribution of the dye, $n_{Cd}(\lambda)$, as given by eqn (5). The coefficients A and B were fitted so that n_{KK} overlaps with the ellipsometry results in the short and long wavelength ranges far from the oscillatory feature in Δn (Table S1 in the SI).

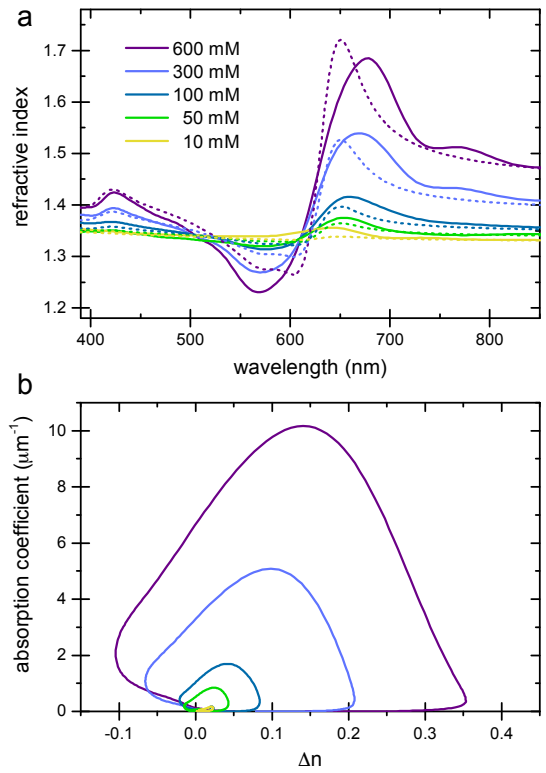


Fig. 3 Refractive index variation of Brilliant Blue solutions in water as a function of dye concentration. (a) Ellipsometry measurements (solid lines) are compared to $n_{KK}(\lambda)$ calculated using the Kramers-Kronig relation (eqn (2), dashed lines). Note the increase in the refractive index at short wavelengths, which is indicative of additional dye absorption peaks below 250 nm (see text)²². (b) A plot of the absorption coefficient vs. Δn clearly reveals a substantial Δn -enhancement in spectral regions where the absorption coefficient is practically zero.

The motivation for the fitting procedure resulting in n_{Cd} stems from the fact that $\kappa(\lambda)$ of the dye is unknown for $\lambda < 250$ nm, the presence of which will give rise to a Cauchy-type decay for $\lambda > 250$ nm. Using this approach, an excellent agreement between calculated and measured refractive index spectra in the visible wavelength range was found (Fig. 2b,d,f,h).

2.3 Refractive index tuning

The refractive index of the liquid can be further tuned by changing the concentration of the dye. Fig. 3a demonstrates that it is possible to precisely dial-in a desired refractive index at a target wavelength, by adjusting the concentration of the Brilliant Blue dye. Fig. 3b clearly demonstrates that Δn -enhancements of up to ≈ 0.35 can be achieved in spectral regions where the absorption coefficient is close to zero. The concentration series in Fig. 3a further gives evidence for the presence of a finite n_{Cd} in the visible. With increasing dye concentration, not only does the oscillatory feature of the refractive index become increasingly pronounced, stemming from the single absorption peak at 630 nm, the “baseline” at 380–400 nm also increases with dye concentration. Fig. 1 illustrates that $\Delta n \rightarrow 0$ for shorter wavelengths compared to the absorption peak. Therefore, the baseline variation indicates the

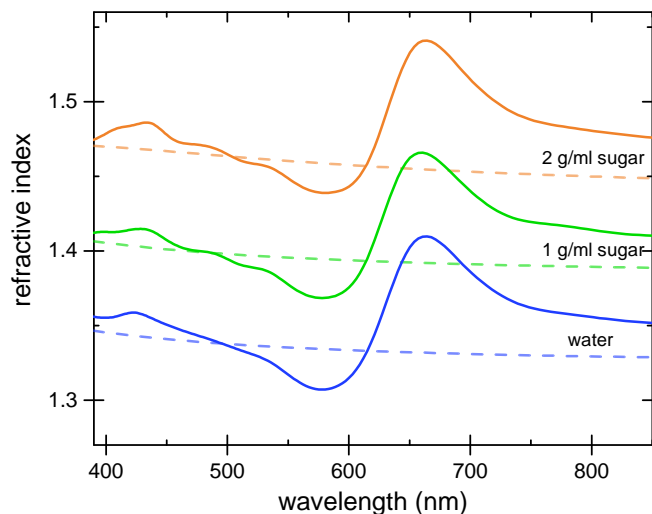


Fig. 4 Refractive index variation of 100 mM Brilliant Blue dissolved in water (bottom curve), 1 g/ml sugar solution (middle curve) and 2 g/ml sugar solution (top curve). The dashed lines show the dye-free reference.

presence of a Cauchy term, eqn (5), stemming from dye absorption peaks below 380 nm.

The comparison of the calculated n_{KK} with the measured ellipsometry spectra is very good, given the fact that spectral information outside the 250–1000 nm wavelength window is missing and Cauchy approximations were employed instead. Note also that while the fit determining $n_{Cd}(\lambda)$ improves the Kramers-Kronig description of the experimental data, the predictive quality of n_{KK} even in the absence of any fitting (i.e. setting $n_{Cd} = 0$) is very good, showing the strength of this approach (Fig. S4 in the SI).

A further way to control the refractive index of a liquid at a given refractive index is the combination of the “traditional” method, the addition of a transparent additive, with the present Kramers-Kronig approach. Fig. 4 shows the measured refractive index spectra of 0.1 M Brilliant Blue dissolved in two sugar solutions. The combination of raising the Cauchy background (eqn (5)) with the Kramers-Kronig response of the dye provides a versatile way to control the refractive index of the solution across large parts of the optical spectrum.

3 Conclusions

In summary, we have harnessed a nearly 100-year old concept in optics for the design of refractive indices in liquids. When employing narrow bandwidth illumination, as e.g. provided by lasers, the well-established Kramers-Kronig relations that link the refractive index with the absorption coefficient provide an approach to specifically dial-in a target refractive index at any narrow wavelength band. Using common food dyes, refractive indices close to 1.7 were obtained. It should be possible to further enhance the refractive index variation by developing dyes that optimise the Kramers-Kronig effect, featuring high absorption coefficients with a sharp long-wavelength decay. Alternatively, it might be possible to suspend organic or inorganic nanoparticles in solution to harness the high extinction coefficients of crystalline materials^{16,23}. Finally, while the refractive index enhancement at long

wavelengths is larger than the refractive index reduction of the Kramers-Kronig oscillation caused by a well-defined absorption peak at shorter wavelengths, this effect can also be employed for the targeted refractive index reduction, e.g. to index match or produce narrow-band anti-reflective coatings.

Conflicts of interest

There are no conflicts of interests to declare.

Acknowledgements

This work was partially funded by the ERC Advanced Grant (H2020-Prismoid, to US) and through the Swiss National Science Foundation through the NCCR *Bio-inspired Materials* (to TS, ERD, US, BDW) and the Ambizione programme (168223, to BDW).

Notes and references

- 1 E. Hecht, *Optics*, Pearson, 2016.
- 2 R. D. Butler, *American Mineralogist: Journal of Earth and Planetary Materials*, 1933, **18**, 386–401.
- 3 J. J. Cargille, *NY Microscop. Soc., Yearbook*, 2008, **9**, year.
- 4 R. L. Darneal, *American Mineralogist: Journal of Earth and Planetary Materials*, 1948, **33**, 346–352.
- 5 R. Meyrowitz and E. S. Larsen Jr, *American Mineralogist: Journal of Earth and Planetary Materials*, 1951, **36**, 746–750.
- 6 C. West, *American Mineralogist: Journal of Earth and Planetary Materials*, 1936, **21**, 245–249.
- 7 M. Guo, P. Chandris, J. P. Giannini, A. J. Trexler, R. Fischer, J. Chen, H. D. Vishwasrao, I. Rey-Suarez, Y. Wu, X. Wu, C. M. Waterman, G. H. Patterson, A. Upadhyaya, J. W. Taraska and H. Shroff, *Nature Methods*, 2018, **15**, 425–428.
- 8 J. M. Laskar, P. S. Kumar, S. Herminghaus, K. E. Daniels and M. Schröter, *Applied Optics*, 2016, **55**, 3165.
- 9 V. Lucarini, J. J. Saarinen, K.-E. Peiponen and E. M. Vartiainen, *Kramers-Kronig relations in optical materials research*, Springer Science & Business Media, 2005, vol. 110.
- 10 H. A. Kramers, *Atti Cong. Intern. Fisica (Transactions of Volta Centenary Congress) Como*, 1927, **2**, 545–557.
- 11 R. de L. Kronig, *J. Opt. Soc. Am.*, 1926, **12**, 547–557.
- 12 H. M. Nussenzveig, *Causality and dispersion relations*, Academic Press, 1972.
- 13 D. J. Faber, M. C. Aalders, E. G. Mik, B. A. Hooper, M. J. van Gemert and T. G. van Leeuwen, *Physical review letters*, 2004, **93**, 028102.
- 14 D. G. Stavenga, H. L. Leertouwer and B. D. Wilts, *Light: Science & Applications*, 2013, **2**, e100–e100.
- 15 D. G. Stavenga and B. D. Wilts, *Philosophical Transactions of the Royal Society B: Biological Sciences*, 2014, **369**, 20130041.
- 16 B. D. Wilts, B. Wijnen, H. L. Leertouwer, U. Steiner and D. G. Stavenga, *Advanced Optical Materials*, 2017, **5**, 1600879.
- 17 F. Jenkins, *Fundamentals of Optics*, McGraw-Hill, New York, 1976.
- 18 G. P. Agrawal, *Nonlinear Science at the Dawn of the 21st Century*, Springer, 2000, pp. 195–211.

- 19 S. Owa and H. Nagasaka, Journal of Micro/Nanolithography, MEMS, and MOEMS, 2004, **3**, 97–104.
- 20 N. Martins, C. L. Roriz, P. Morales, L. Barros and I. C. Ferreira, Trends in Food Science & Technology, 2016, **52**, 1–15.
- 21 R. Synowicki, G. K. Pribil, G. Cooney, C. M. Herzinger, S. E. Green, R. H. French, M. K. Yang, J. H. Burnett and S. Kaplan, Journal of Vacuum Science & Technology B: Microelectronics and Nanometer Structures Processing, Measurement, and Phenomena, 2004, **22**, 3450–3453.
- 22 Compared to the trend given by the lower dye concentrations, the experimental curve of the 600 mM Brilliant Blue solution has a lower than expected refractive index maximum. Since this concentration is close to the solubility limit, a small fraction of the dye may have separated from the solution cause an effective solution concentration below 600 mM. By extrapolation the probable solution concentration of this data set was 540 mM.
- 23 B. A. Palmer, V. J. Yallapragada, N. Schiffmann, E. M. Wormser, N. Elad, E. D. Aflalo, A. Sagi, S. Weiner, L. Addadi and D. Oron, Nature Nanotechnology, 2020, 1–7.

Designing Refractive Index Fluids using the Kramers–Kronig Relations

– Supplementary Information –

Tianqi Sai,^{a,b} Matthias Saba,^a Eric R. Dufresne,^b Ullrich Steiner,^{*a} and Bodo D. Wilts^{*a}

^a Adolphe Merkle Institute, University of Fribourg, Chemin des Verdiers 4, CH-1700 Fribourg, Switzerland. E-mail: ullrich.steiner@unifr.ch; bodo.wilts@unifr.ch

^b Department of Materials, ETH Zürich, Vladimir-Prelog-Weg 5, CH-8093 Zürich, Switzerland.

Materials and methods

Materials

The four dyes Brilliant Blue, Allura Red, Pyranine and Quinoline Yellow were purchased from fastcolours.com. Their chemical structures and IUPAC full names are given in Fig. S1. Stock solutions with concentrations of 600 mM for Brilliant Blue and 300 mM for the other dyes were prepared and subsequently diluted to lower concentrations. The absorption of those dyes in the visible range is mainly due to the resonance among the benzene rings and double bonds in the structures*.

Optical characterization

Transmittance spectra were recorded using a spectrometer (Maya Pro, Ocean Optics) with a wavelength range from 250 – 1000 nm. The dye solutions were filled into a quartz cuvette with a 1 cm light path and then placed into a Thorlabs CVH100 cuvette holder, which has two fiber adapters on opposite sides. Light from a halogen/deuterium or a xenon light source (DHL-Bal or HPX-2000, both Ocean Optics) passes through the sample and is guided into the spectrometer via optical fibres with a 200 μm diameter (QP200-2-SR-BX, Ocean Optics). A water-filled cuvette was used as reference.

Assuming a small extinction coefficient $\kappa \ll n$, the absorption coefficient α is experimentally measured through application of the Beer-Lambert law

$$\frac{I(\lambda)}{I_0(\lambda)} = e^{-i\alpha(\lambda)d}, \quad (\text{S1})$$

with I , I_0 the transmitted intensities of light after passing through a dye solution of thickness d and a dye-free reference, respec-

tively. The molar absorption coefficient is then defined as

$$\varepsilon(\lambda) = \frac{\alpha(\lambda)}{c_d}, \quad (\text{S2})$$

where c_d is the molar concentration of the dye. The relation to the extinction coefficient κ is given by eqn (4).

Refractive index measurements

The refractive index dispersion was measured with an optical ellipsometer (alpha-se, JA Wollam). For this, the liquid was deposited onto rough, frosted glass slides (Marienfeld) and the dielectric function was extracted as described previously by Synowicki *et al.*²¹.

The refractive index of the fluids was additionally assessed with an automatic refractometer (Abbemat MW, Anton-Paar) at six discrete wavelengths (455.0 nm, 488.0 nm, 513.3 nm, 533.1 nm, 589.3 nm and 644.2 nm), with a RI range of 1.30 - 1.72 nD and an accuracy of ± 0.00004 nD.

dye	A	B [nm ²]
Brilliant Blue	0.064 ± 0.008	0
Allura Red	0.062 ± 0.004	511 ± 25
Pyranine	0.0143 ± 0.001	946 ± 31
Quinoline Yellow	0.0393 ± 0.003	2258 ± 69

Table S1 Fit parameters A , B , determining $n_{Cd}(\lambda)$ according to eqn (5) for the four dyes.

* A. Gürses, M. Açıkyıldız, K. Güneş, Kübra and M. S. Gürses, Dyes and Pigments, Springer, 2016, pp. 31â$45.

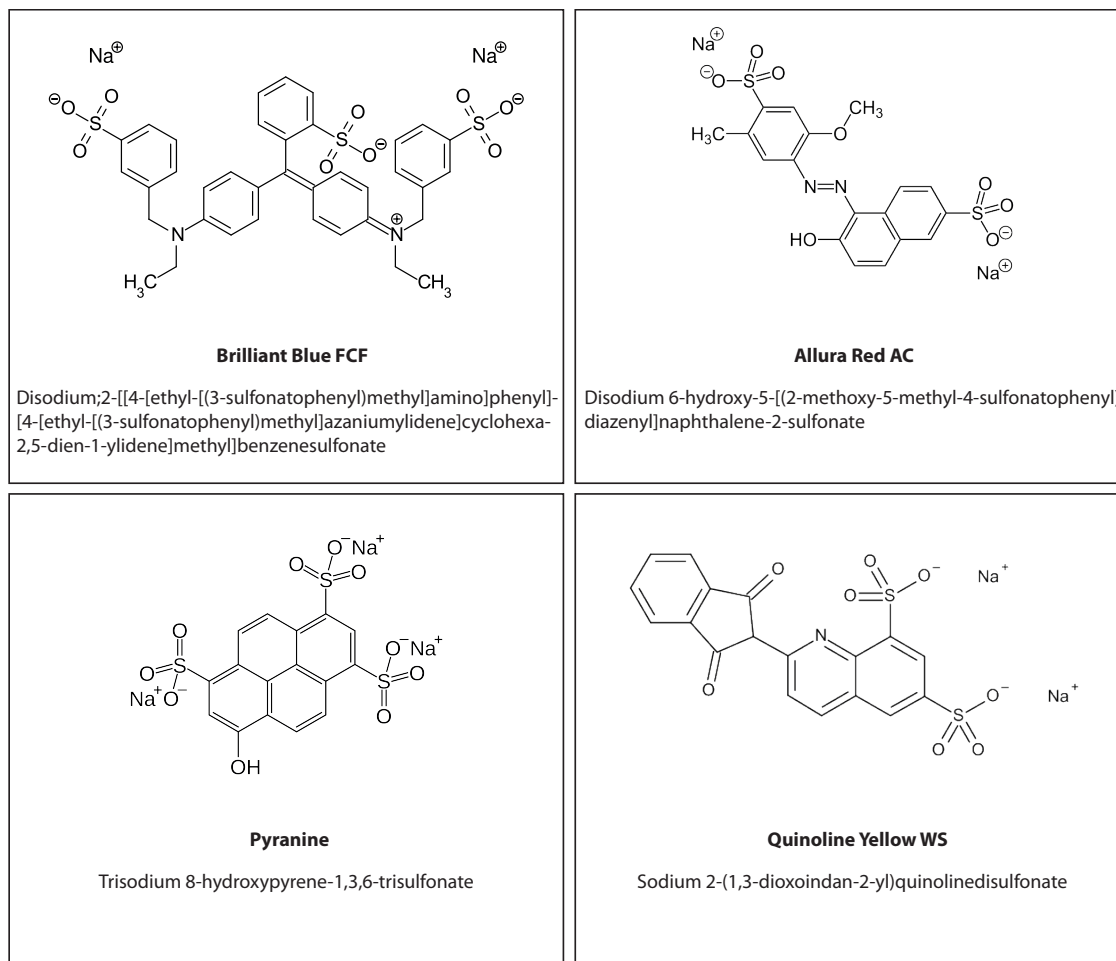


Fig. S1 Chemical structures and IUPAC names of the dyes used in this study

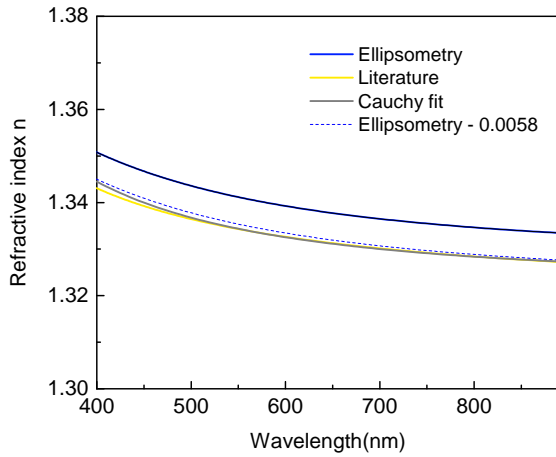


Fig. S2 Ellipsometry measurement of the refractive index of water, in comparison with literature values. In this study, a Cauchy fit (eqn (5)) was used to account for the spectral variation of the refractive index of water. Despite the close agreement of the dispersion curve from literature and the ellipsometry measurements, an offset of 0.0058 was deducted from all ellipsometry measurements to account for the discrepancy found in this measurement.

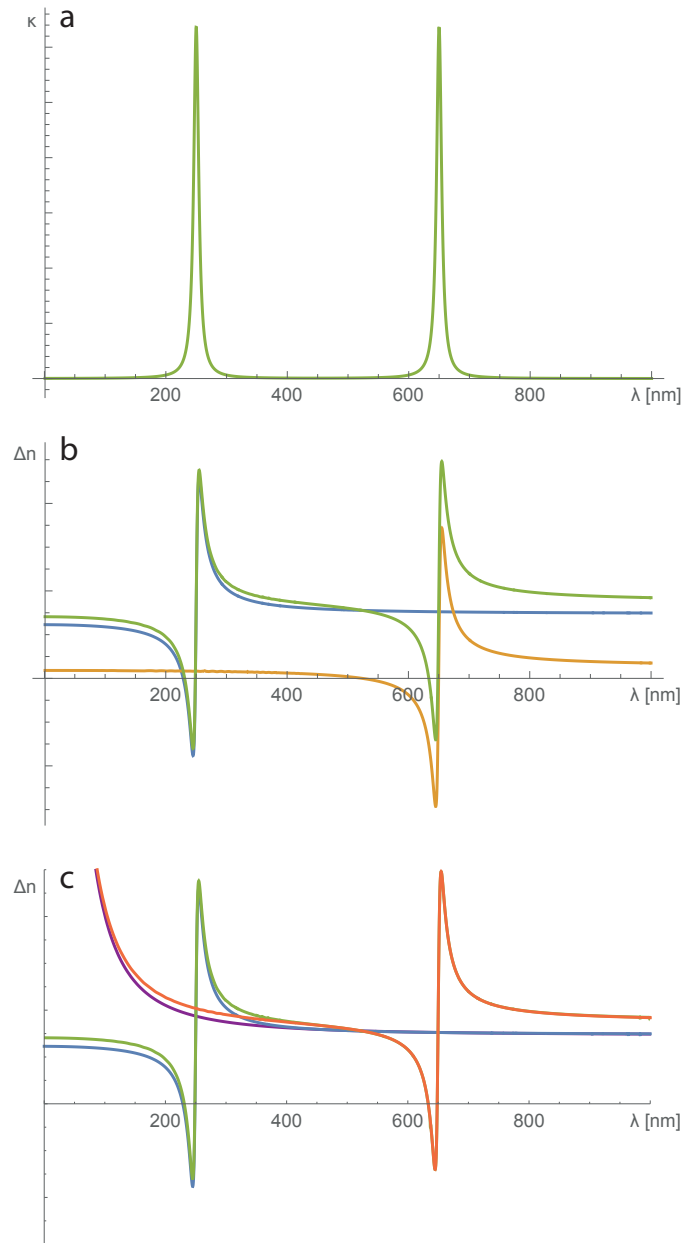


Fig. S3 Model calculations illustrating the additivity of the results of eqn (2). (a) Hypothetical extinction spectrum consisting of two Lorentz distributions centred at 250 nm and 650 nm. (b) The integration of eqn (2) of extinction spectra containing each peak separately result in the orange and blue lines, which were added to yield the green spectrum. This resulting green spectrum is indistinguishable from the one stemming from an integration employing the double-peak spectrum. In (c) the Cauchy equation eqn (5) was fitted to the blue spectrum for wavelengths greater than 400 nm, resulting in the purple line. The addition of this Cauchy spectrum with the orange line in (b) (resulting from the Kramers-Kronig integration of only the right peak) gives rise to the red line in (c), which approximates the exact spectrum (green line) very closely for wavelengths above 400 nm.

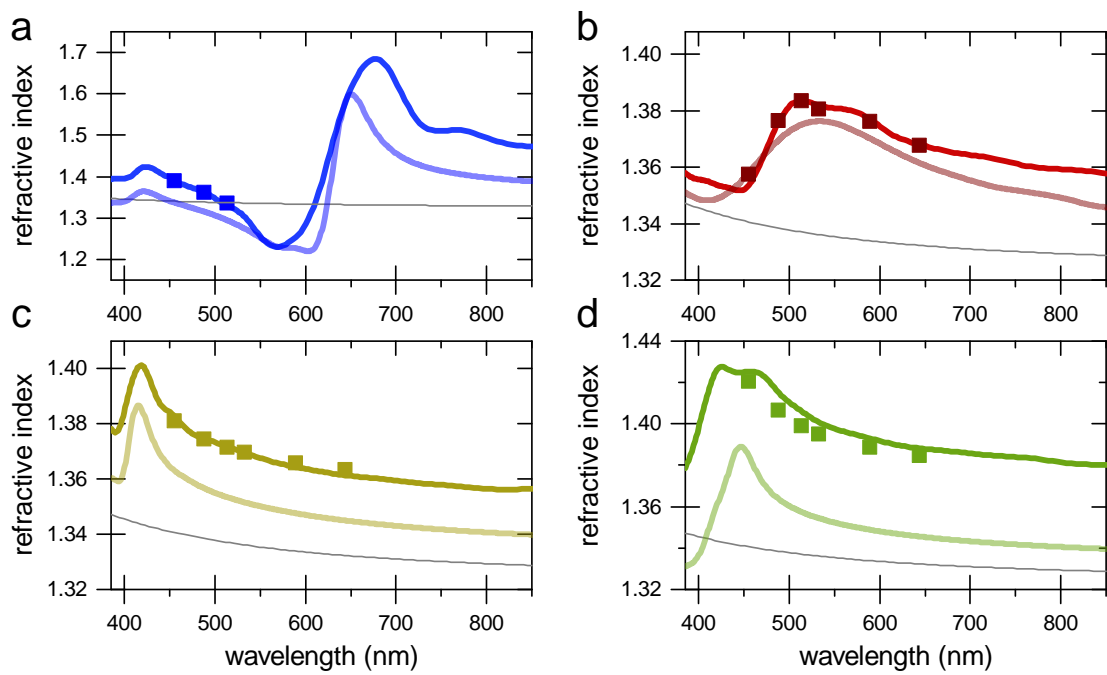


Fig. S4 Refractive index data from Fig. 2 (solid lines) and the predictions of Kramers-Kronig relation n_{KK} (light coloured lines). In the calculation of n_{KK} only the Cauchy correction for water n_{Cw} was taken into account and the final Cauchy fit was omitted ($n_{Cd} = 0$, see text).